Fault Delineation using Spectral Decomposition of Relative Acoustic Impedance Data and RGB Blending

Vikas Saluja, Uday Singh, Aninda Ghosh, Puja Prakash, Rajeev Verma and H K Singh
vikaspes@yahoo.com

Keywords

Fault Delineation, Spectral Decomposition, Relative Acoustic Impedance, RGB Blending

Summary

The case study demonstrated here is the innovative workflow for fault delineation technique on a 3D seismic volume in B-173A Field of Heera Panna Bassein (HPB) Sector, Western Offshore Basin, India. B-173A is located 50 kms west of Mumbai at an average water depth of about 50 m. The field was discovered in the year 1992 and it was put on production in Aug 1998. In B-173A field there are two hydrocarbon bearing zones one is gas bearing Mukta (Lower Oligocene carbonates) Formation and oil bearing Bassein (Middle to Upper Eocene Carbonates) formation.

The present study is an innovative workflow on Advanced Seismic Interpretation using Spectral Decomposition and RGB Blending for Fault delineation. Iso-frequency volumes are extracted from Relative Acoustic Impedance data instead of seismic data itself.

The workflow is for effective fault delineation and it consists of Spectral Decomposition of relative acoustic impedance data and RGB Blending of discontinuity attributes of different Iso-frequency volumes.

It is observed that RGB blend volume of discontinuity attributes provided more convincing results for fault delineation as compared to the results of traditional discontinuity attributes.

Introduction

Area Overview

B-173-A field (Fig. 1) is part of Heera Panna Bassein (HPB) sector that lies in eastern part of the Western Offshore basin. On the east of HPB sector lies Eastern Homocline, Murud Low and Mumbai High is on the west, Tapti Daman to the north and Ratnagiri Block is on the south. Hydrocarbon occurrence in this sector is established from Panna, Bassein, Mukta,

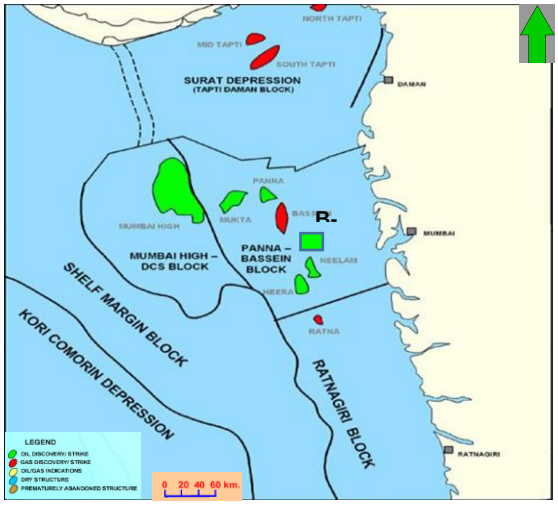

Figure 1: Index Map of Western Offshore Basin

Heera and Bandra formations of Early Eocene to Miocene age. Minor oil accumulation is also observed in Basement.

In B-173A field, the most prolific carbonate reservoirs are Mukta and Bassein Formations. The Mukta Formation (H3A) thickness 25-60m is having alternation of carbonate and shale throughout the area with established gas in B-173A field and oil in NW-B-173A field.

In the Eastern Homoclinal area, the migration of hydrocarbons from the Central graben has been in the updip direction to the crestal areas. The migration would have been along the normal faults and further migration is expected to take place till a lateral seal is encountered in the form of porosity barrier. The shales below Mukta Formation are envisaged to provide the vertical seal for Bassein and shales of Heera Formation are envisaged to provide the vertical seal for Mukta Fm.

Western Offshore Basin is characterized by three sets of longitudinal extensional fault giving rise to a series

Fault Delineation using Spectral Decomposition of Relative Acoustic Impedance Data and RGB Blending

of horst and graben features. The fault pattern is primarily guided by three primordial tectonic trends: Delhi-Aravalli (NE-SW), Dharwar (NNW-SSE) and Satpura (ENE-WSW).

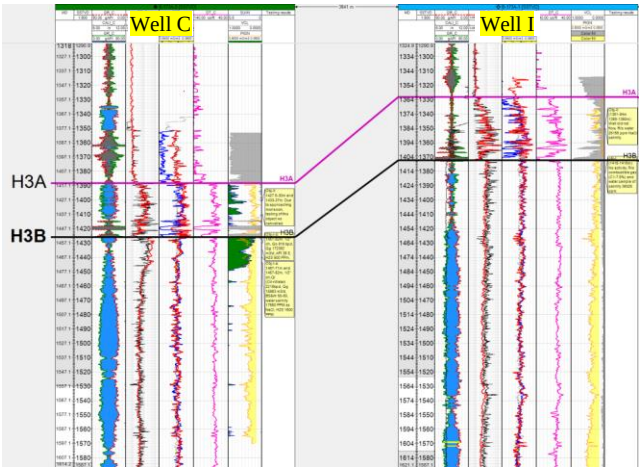

Figure 2: Log-Correlation profile along Well C and Well I

The well C of B-173A field is oil bearing in Bassein Formation. The well I having good facies development and being structurally shallower position is water bearing in Mukta as well as in Bassein Formation (Fig. 2). These wells are separated by a fault, which acted as a barrier. Wells H & I drilled in NE of fault show good facies development but devoid of hydrocarbon fault, whereas wells C and E in SW are hydrocarbon bearing and well D, F G are below the established water contact. Therefore, fault mapping is vital to understand the hydrocarbon entrapment in the B-173A field.

History of Fault Delineation Algorithms

Discontinuity attributes are applied to stacked migrated seismic data volumes to facilitate the interpretation of geologic structural or stratigraphic discontinuities. In general, such attributes are extracted from stacked data after migration, and is available in most workstation interpretation software packages. Various implementations of discontinuity attribute algorithms have evolved over the last 25 years including cross correlation-based (Bahorich and Farmer, 1995), semblance-based (Marfurt et al., 1998), variance-based (Pepper and Bejarano, 2005), Sobel filter based (Luo et al., 1996, 2003), eigen structure-based (Gersztenkorn and Marfurt, 1999), gradient structure tensor-based (Bakker, 2003) and Amplitude-volume technique based (Vernengo and Trinchero, 2015) algorithms. Details about the applications of coherence attribute to seismic data is discussed in Chopra and Marfurt, (2007, 2018a, 2018b).

The interpretation of stratigraphic features on seismic data is dependent on their bandwidth. In general, seismic data that have a higher bandwidth also provide greater lateral resolution, resulting in sharper discontinuity images. For these reasons, sometimes interpreters run spectral decomposition (Partyka et al., 1999) prior to computing discontinuity attribute (Chopra and Marfurt, 2016). In general, higher frequency spectral magnitudes highlight lateral variation in thinner beds while lower frequency magnitude highlights lateral changes in thicker beds. Another tool at their disposal is the red-green-blue (RGB) blending (Henderson et al., 2008) of three frequency components, which allows interpreters to co-render the information content at different scales.

Obviously, if a given spectral component highlights a feature of interest, one can delineate edges in such volumes using coherence. The same argument applies to azimuthally limited, offset-limited, or angle-limited partial stacks of the migrated data. Because of AVO effects, lithologic “edges” may be stronger on coherence computed on the far-offset stack. Similarly, faults and other discontinuities will be better illuminated by a perpendicular rather than a parallel azimuthally-limited partial stack (Chopra and Marfurt, 2007). Unfortunately, there are two major drawbacks to this “component analysis” workflow. First, each spectral component or partial stack has a lower signal-to-noise content than the broadband or full stack data volume. Second, the interpreter is now faced with interpreting multiple coherence images, one for each component, which (because of their lower signal-to-noise ratio) can be both tedious and very time consuming.

As different spectral components are sensitive to different scales of discontinuities, the challenge is to analyze these volumes effectively. Alternative methods that can be used for this purpose include using RGB color blending, principal component analysis (PCA), self-organizing maps (SOMs) and multispectral coherence.

Marfurt (2017) describes a way to construct a multispectral covariance matrix by summing the covariance matrices for all the input spectral components each of which is oriented along

Fault Delineation using Spectral Decomposition of Relative Acoustic Impedance Data and RGB Blending

structural dip using analytic voice components. The energy ratio coherence computed using this approach is referred to as multispectral coherence. Qi et al. (2017) extended this concept to azimuthally-limited and offset-limited partial stacks, resulting in "multiazimuth" and "multioffset" coherence (Chopra and Marfurt, 2019).

PCA (principal component analysis) is based on the statistical assumption that the input multivariate data exhibit a Gaussian distribution. Principal component analysis is a good dimensionality reduction tool. Maximum information is represented by the most important eigenvectors.
Computation of various discontinuity attributes is based on the variation in amplitude, frequency, dip and waveform shape. And many a times, these attributes provide redundant information such as output of different fault delineation algorithms or discontinuity attributes computed on various iso-frequency volumes. PCA is useful to get rid of the redundant information during multi-attribute analysis. The first eigenvector (i.e. first principal component) corresponding to the highest eigen-value represents the maximum variability in the scaled attributes, while the second principal component is the eigenvector corresponding to the second-highest eigenvalue which reveals the lower variance. Similarly, the third principal component will exhibit much lower variance than the second principal component. All these principal components are orthogonal to each other. As these seismic attributes are representing the discontinuity of subsurface strata, the first two or three principal components will almost exhibit the maximum variability present in the multi-attributes (Chopra and Marfurt, 2014).
Combining discontinuity attributes computed from different iso-frequency volumes using PCA could be a better option for fault delineation as analysis of multiple attributes one by one is a tedious and time taking job. Ideally first one or two principal components will represent the maximum variability present in the multi-attributes. PCA reduces the dimensionality in terms of the number of attributes we want to utilize and it may be useful for the interpreter.

RGB color blending of three different data sets is an effective way of incorporating all the information present in the individual attributes for ease in comparison, viewing, and so in interpretation. Leppard et al. (2010) and Henderson et al. (2008) given excellent examples of effective RGB color blending to represent three different spectral components.
The algorithms most commonly available on software packages are the semblance and some form of Eigen structure decomposition of covariance matrices. Algorithms for multi-spectral, multi-offset and multi-azimuth coherence are yet to come on commercial S/W. RGB color blending and Machine learning algorithms such as PCA are easily available in industry S/W which can be used for effective fault delineation.
The workflow adopted here consists of Spectral Decomposition of relative acoustic impedance data and RGB blending of discontinuity attributes of different Iso-frequency volumes.

Methodology

The innovative workflow consists of Spectral Decomposition of Relative Acoustic Impedance data & RGB blending of discontinuity attributes of different Iso-frequency volumes for fault delineation. The workflow is:
1. Compute RAI (Relative Acoustic Impedance) on 3D Seismic Data
2. Perform Spectral Decomposition and generate iso-frequency volumes
3. Compute discontinuity attribute on each iso-frequency volume
4. RGB blending of various discontinuity attributes derived from step 3 of for fault delineation

Sections passing through well C and I from Seismic volume, RAI volume and 60 Hz frequency volume are shown in Fig. 3, 4 and 5. The fault between these two wells is clearly visible on seismic section. But the same fault (marked with yellow color) is very subtle in the traditional discontinuity attribute time slice (Fig. 6) at 1370 ms and to enhance this fault using the existing seismic data, above workflow (Fig. 7) has been adopted.

The discontinuity attributes were computed from iso-frequency volumes of 40, 50 & 60 Hz. It is observed that discontinuity run on spectrally decomposed volumes, especially the ones at higher frequencies within the seismic bandwidth, exhibit higher lateral

Fault Delineation using Spectral Decomposition of Relative Acoustic Impedance Data and RGB Blending

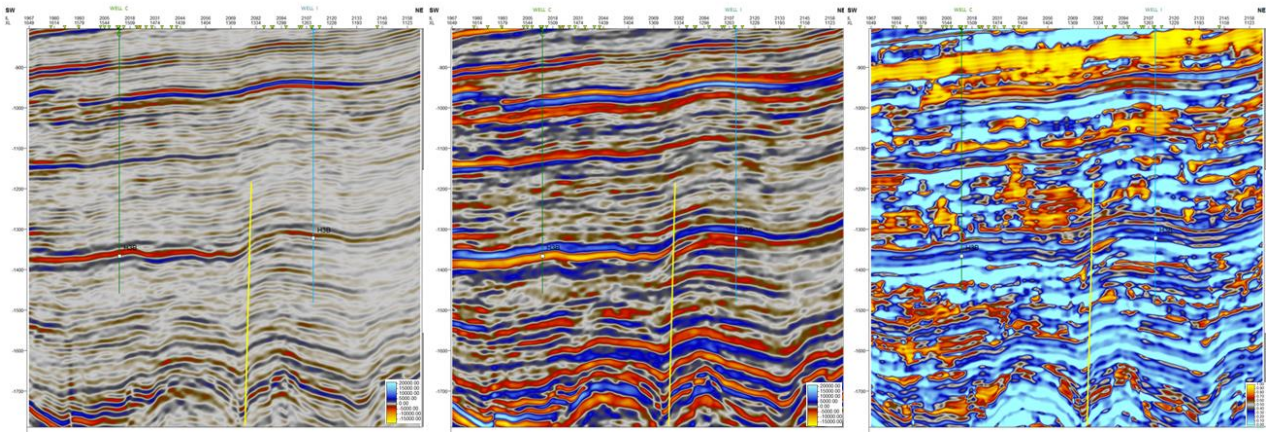

Sections passing through well C and I from Seismic volume (Figure 3), RAI volume (Figure 4) and 60 Hz Frequency volume (Figure 5)

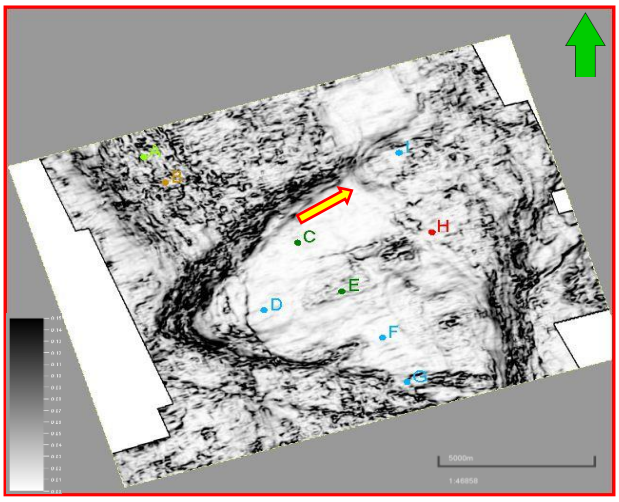

Figure 6: Discontinuity Slice of Seismic data at 1370 ms

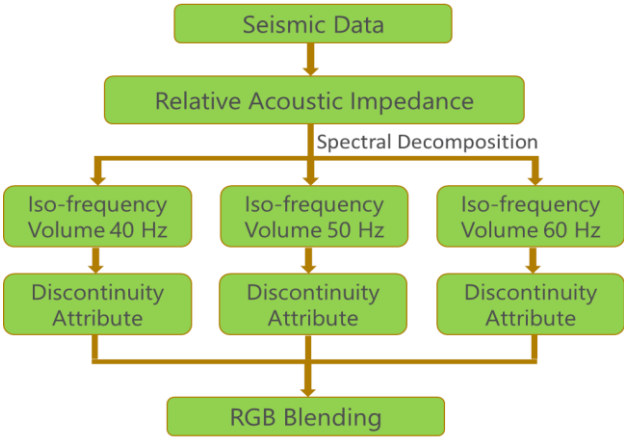

Figure 7: Workflow for Fault Delineation

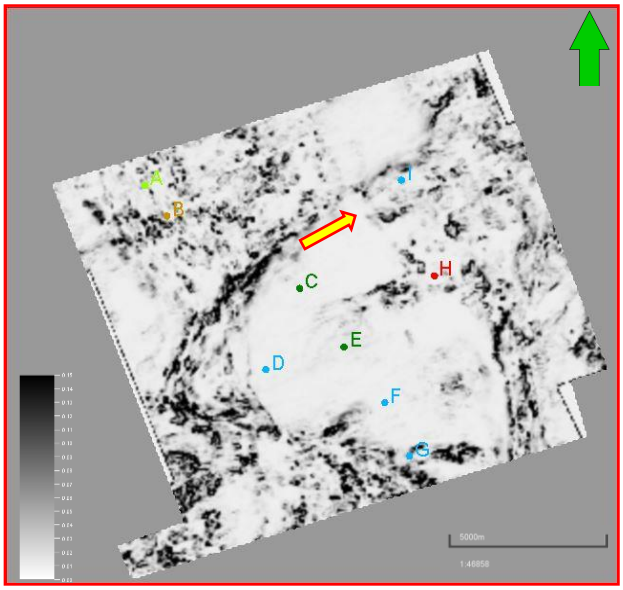

Figure 8: Discontinuity Slice from 40Hz Iso-frequency volume at 1370ms

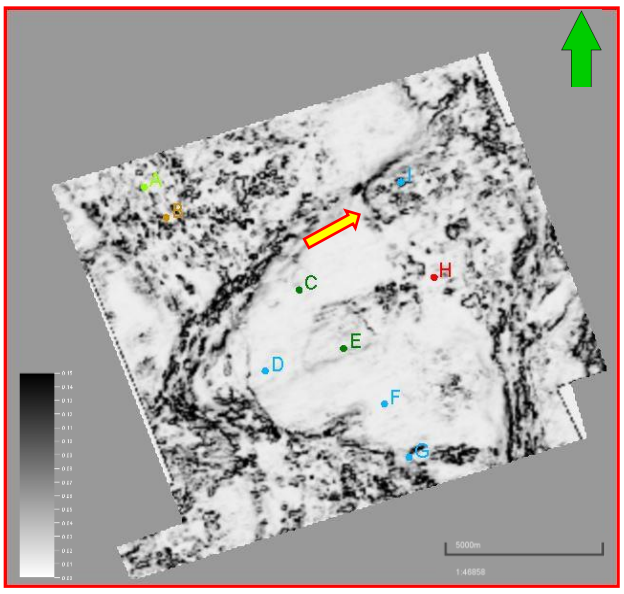

Figure 9: Discontinuity Slice from 50Hz Iso-frequency volume at 1370ms

Fault Delineation using Spectral Decomposition of Relative Acoustic Impedance Data and RGB Blending

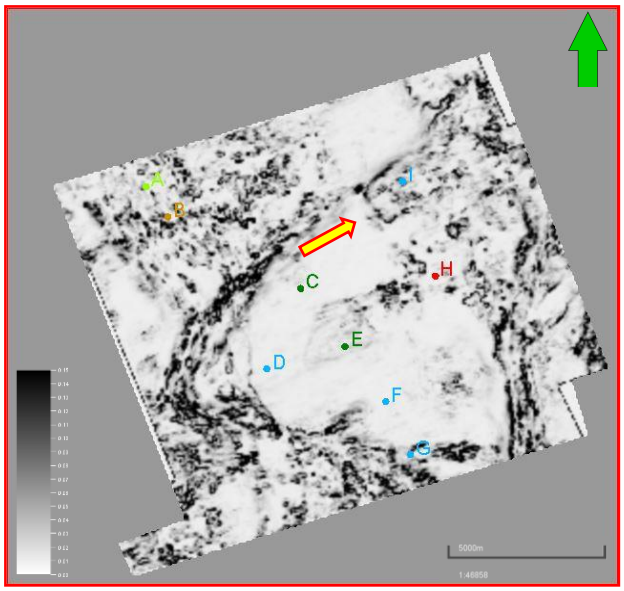

Figure 10: Discontinuity Slice from 60Hz Iso-frequency volume at 1370ms

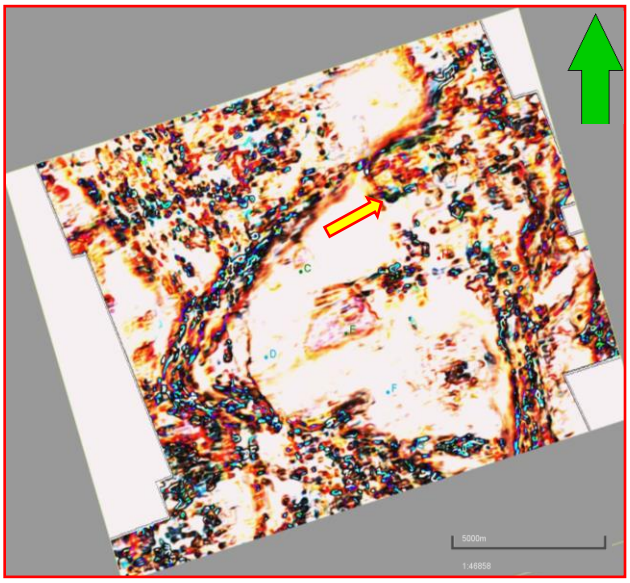

Figure 11: Slice derived from RGB blended volume at 1370 ms

resolution as comparison to conventional post stack discontinuity volume. The Fault (marked with yellow arrow) shown in discontinuity attributes of iso-frequencies volumes (corresponding to 40, 50 & 60 Hz) is well defined (Fig. 8,9 and 10) as compared to the discontinuity attribute calculated from original seismic data (Fig. 6).

For better delineation, discontinuity attributes of iso-frequency volumes (40, 50 and 60 Hz) of RAI (Relative Acoustic Impedance) was used as input for RGB blending. RGB blended volume was generated and it was observed that the same fault (marked with yellow arrow) is more clearly defined in the RGB blended volume (Fig. 11) as compared to conventional discontinuity attribute of seismic data (Fig. 7).

Conclusions

Iso-frequency volume corresponding to the higher frequency enhance the discontinuities in the data. Discontinuity attribute on iso-frequency volumes highlights the discontinuities at different frequencies. Combining discontinuity attributes derived from different iso-frequency volumes using color is an effective way of combining the multiple attributes, but it is limited to three colors only.

Here the comparison is shown between fault delineation using conventional discontinuity attribute and RGB blending of derived attributes from discontinuity attributes of different Iso-frequency volumes of RAI (Relative Acoustic Impedance) calculated from same seismic data and it is observed that RGB blended volume delineate the particular fault more effectively as compared to conventional discontinuity volume.

Acknowledgements

Authors are thankful to ONGC for permitting to publish the work. However, the views expressed in the paper are those of the authors only. The authors are indebted to Shri Pradipta Mishra, ED-HOI-GEOPIC and Shri A.C. Naithani, GGM-Head-INTEG-GEOPIC for according permission, providing infrastructural facilities, continuous guidance and inspiration in the study.

References

Bahorich, M. S., and S. L. Farmer, 1995, 3-D seismic coherency for faults and stratigraphic features: The Leading Edge, 14, 1053–1058.

Bakker, P., 2003, Image structure analysis for seismic interpretation: Ph.D. thesis, Technische Universiteit Delft.

Fault Delineation using Spectral Decomposition of Relative Acoustic Impedance Data and RGB Blending

Chopra Satinder et al., 2013, Spectral Decomposition's Analytical Value: Geophysical Corner, Explorer, December, 50-51.

Chopra, S., and K. J. Marfurt, 2007, Seismic attributes for prospect identification and reservoir characterization, Geophysical Development Series, SEG.

Chopra, S., and K. J. Marfurt, 2014, Churning seismic attributes with principal component analysis, Annual International Meeting, SEG, Expanded Abstracts,2672-2676.

Chopra, S. and K. J. Marfurt, 2016, Spectral decomposition and spectral balancing of seismic data, The Leading Edge, 26, 936-939.

Chopra, S. and K. J. Marfurt, 2018a, Coherence attribute applications on seismic data in various guises - Part 1, Interpretation, August, T521-T529.

Chopra, S. and K. J. Marfurt, 2018b, Coherence attribute applications on seismic data in various guises - Part 2, Interpretation, August, T531-T541.

Chopra, S. and K. J. Marfurt, 2019, Multispectral, multiazimuth and multioffset coherence attribute applications, Interpretation, May, SC21–SC32.

Gersztenkorn, A. and K. J. Marfurt, 1999, Eigen structure-based coherence computations as an aid to 3D structural and stratigraphic mapping: Geophysics, 64, 1468-1479.

Henderson, J., S. Purves, G. Fisher, and C. Leppard, 2008, Delineation of geological elements from RGB color blending of seismic attribute volumes: The Leading Edge, v.27/3, p. 342–350.

Honorio, B. C. Z., M. C. de Matos, and A. C. Vidal, 2017, Similarity attributes from differential resolution components: Interpretation, 5, no. 1, T65–T73, doi: 10.1190/INT-2015-0211.1.

Leppard, C., A. Eckersly, and S. Purves, 2010, Quantifying the temporal and spatial extent of depositional and structural elements in 3D seismic data using spectral decomposition and multi attribute RGB blending, in L. J. Wood, T. T. Simo, and N. C. Rosen, eds., Seismic imaging of depositional and geomorphic systems: 30th Annual GCSSEPM Foundation Bob F. Perkins Research Conference: GCSSEPM, 1–10.

Li, F. Y., and W. K. Lu, 2014, Coherence attribute at different spectral scales: Interpretation, 2, no. 1, SA99–SA10, doi: 10.1190/INT-2013-0089.1

Luo, Y., S. al-Dossary, M. Marhoon, and M. Alfaraj, 2003, Generalized Hilbert transform and its application in geophysics: The Leading Edge, 22, 198-202.

Luo, Y., W. G. Higgs, and W. S. Kowalik, 1996, Edge detection and stratigraphic analysis using 3-D seismic data: 66th Annual International Meeting, SEG, Expanded Abstracts,324–327.

Marfurt, K. J., R. L. Kirlin, S. H. Farmer, and M. S. Bahorich, 1998, 3-D seismic attributes using a running window semblance-based algorithm: Geophysics, 63, 1150–1165.

Marfurt, K. J., 2017, Interpretational aspects of multispectral coherence: 79th Annual EAGE Conference and Exposition, Expanded Abstract, Th A4 11.

Partyka, G.A., J. Gridley, and J. Lopez, 1999, Interpretational applications of spectral decomposition in reservoir characterization: The Leading Edge, 18, 353-360.

Pepper, R., and G. Bejarano, 2005, "Advances in seismic fault interpretation automation, AAPG Search and Discovery Article 40170."

Qi, J., F. Li and K. J. Marfurt, 2017, Multiazimuth coherence, Geophysics, 82, P083-089

Vernengo, L., and E. Trinchero, 2015, Application of amplitude volume technique attributes, their variations, and impact: The Leading Edge, 34, 1246–1253, doi: 10.1190/tle34101246.1